

# Observations and modelling of glyoxal in the tropical Atlantic marine boundary layer

Hannah Walker,<sup>1,2</sup> Daniel Stone,<sup>2</sup> Trevor Ingham,<sup>2,3</sup> Sina Hackenberg,<sup>4</sup> Danny Cryer,<sup>2</sup> Katie Read,<sup>4,5</sup> James Lee,<sup>4,5</sup> Lisa Whalley,<sup>2,3</sup> Dominick V. Spracklen,<sup>1</sup> Lucy J. Carpenter,<sup>4</sup> Stephen R. Arnold,<sup>1,\*</sup> Dwayne E. Heard<sup>2\*</sup>

<sup>1</sup> *School of Earth and Environment, University of Leeds, Leeds, LS2 9JT, UK*

<sup>2</sup> *School of Chemistry, University of Leeds, Leeds, LS2 9JT, UK*

<sup>3</sup> *National Centre for Atmospheric Science, School of Chemistry, University of Leeds, Leeds, LS2 9JT, UK*

<sup>4</sup> *Wolfson Atmospheric Chemistry Laboratory, Department of Chemistry, University of York, Heslington, York, YO10 5DD, UK*

<sup>5</sup> *National Centre for Atmospheric Science, Wolfson Atmospheric Chemistry Laboratory, Department of Chemistry, University of Leeds, Leeds, LS2 9JT, UK*

\* Corresponding authors: [s.arnold@leeds.ac.uk](mailto:s.arnold@leeds.ac.uk), [d.e.heard@leeds.ac.uk](mailto:d.e.heard@leeds.ac.uk)

## Supplementary Information

	Page
Figure S1	S2
Figure S2	S5
Figure S3	S8
Figure S4	S8
Figure S5	S9
Figure S6	S10
Figure S7	S11
Figure S8	S11
Figure S9	S12
Figure S10	S12

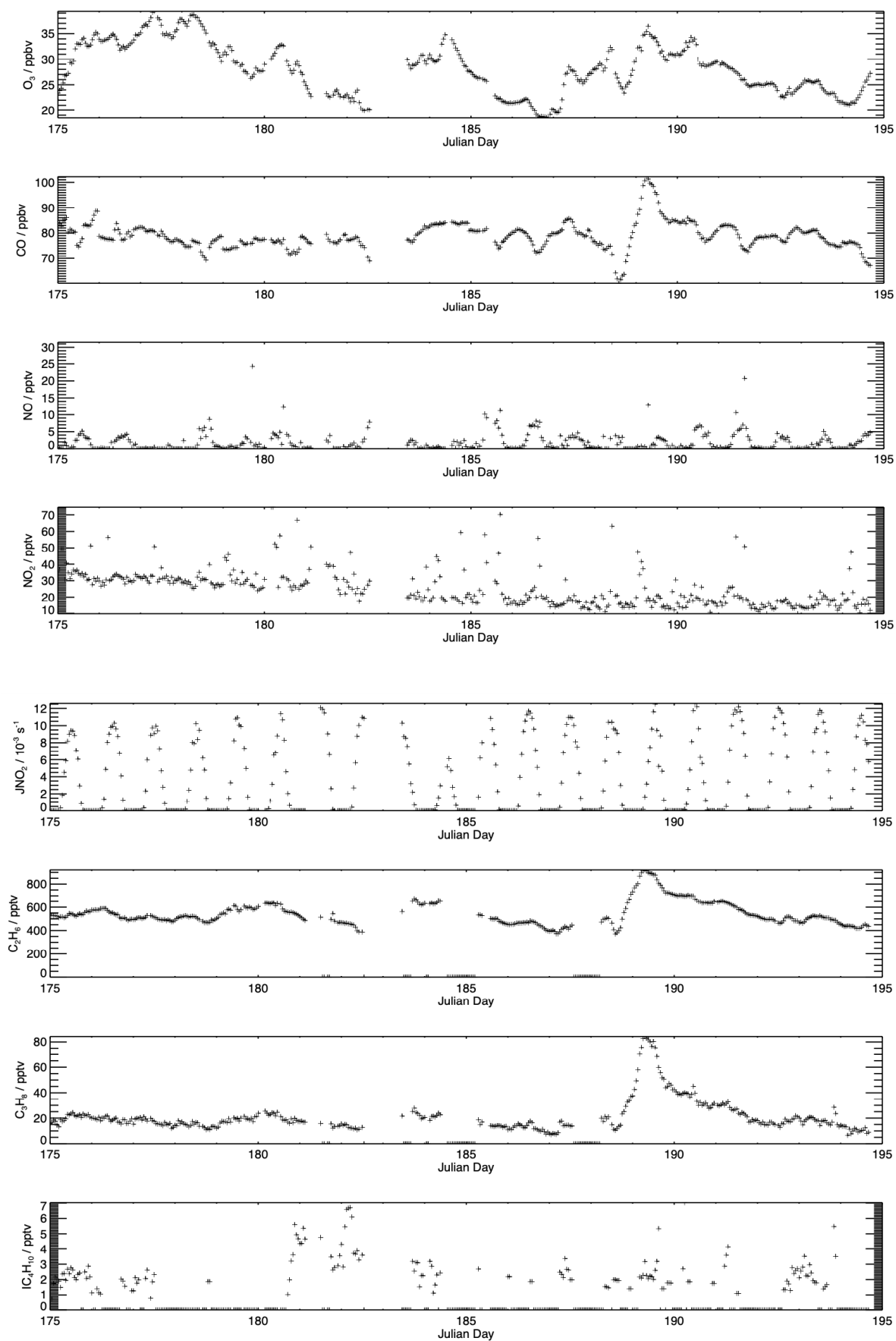


Figure S1: MCM model inputs for campaign 1.

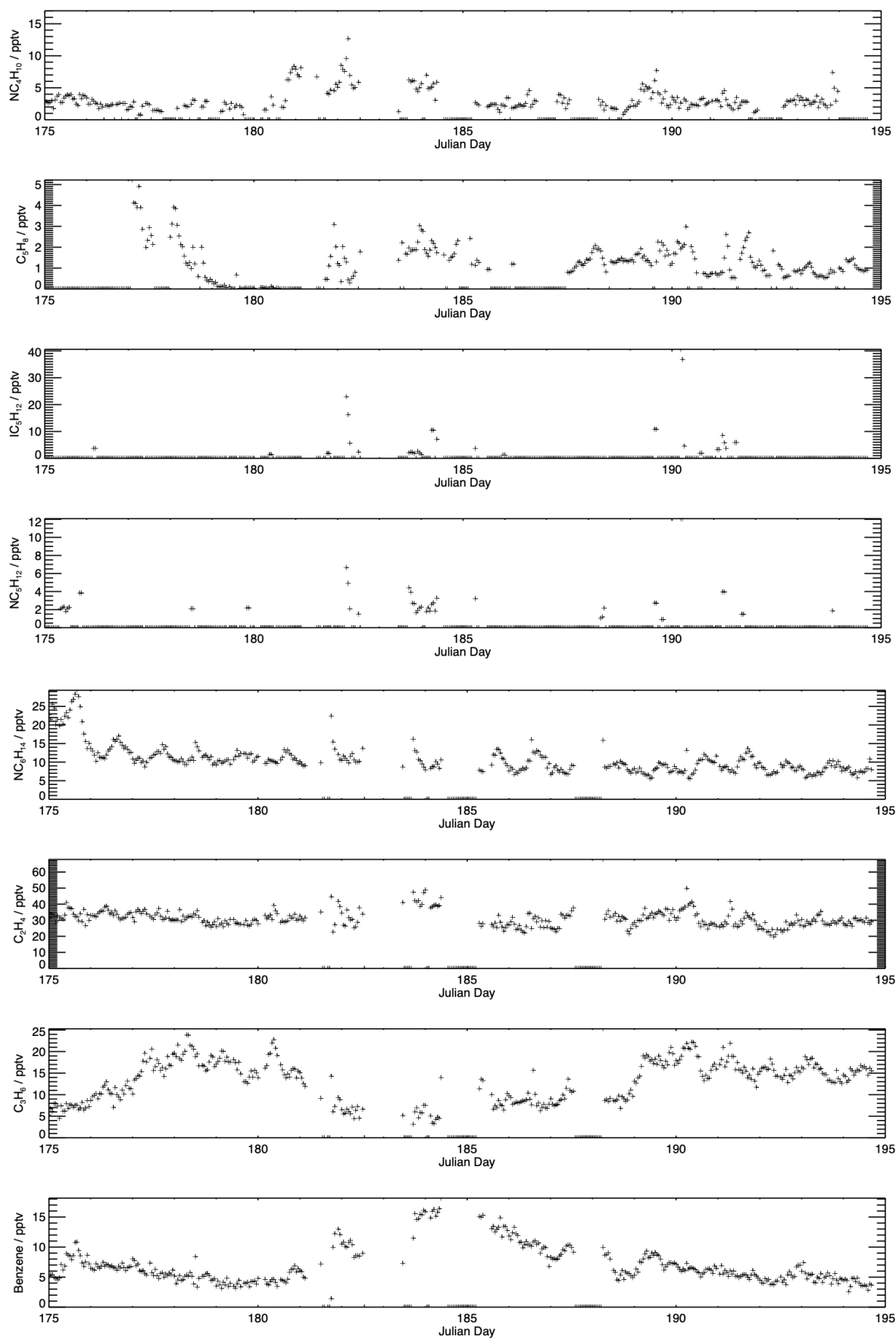


Figure S1: MCM model inputs for campaign 1 (continued).

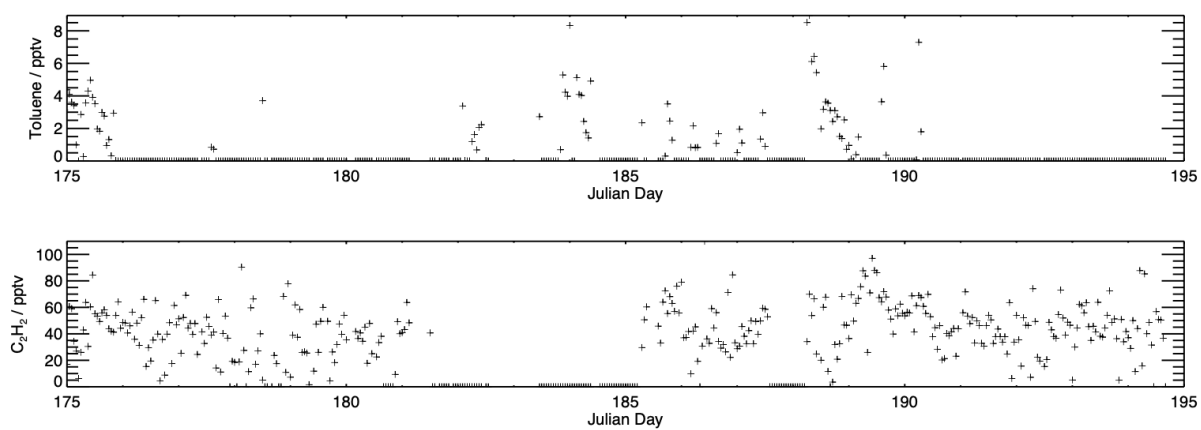


Figure S1: MCM model inputs for campaign 1 (continued).

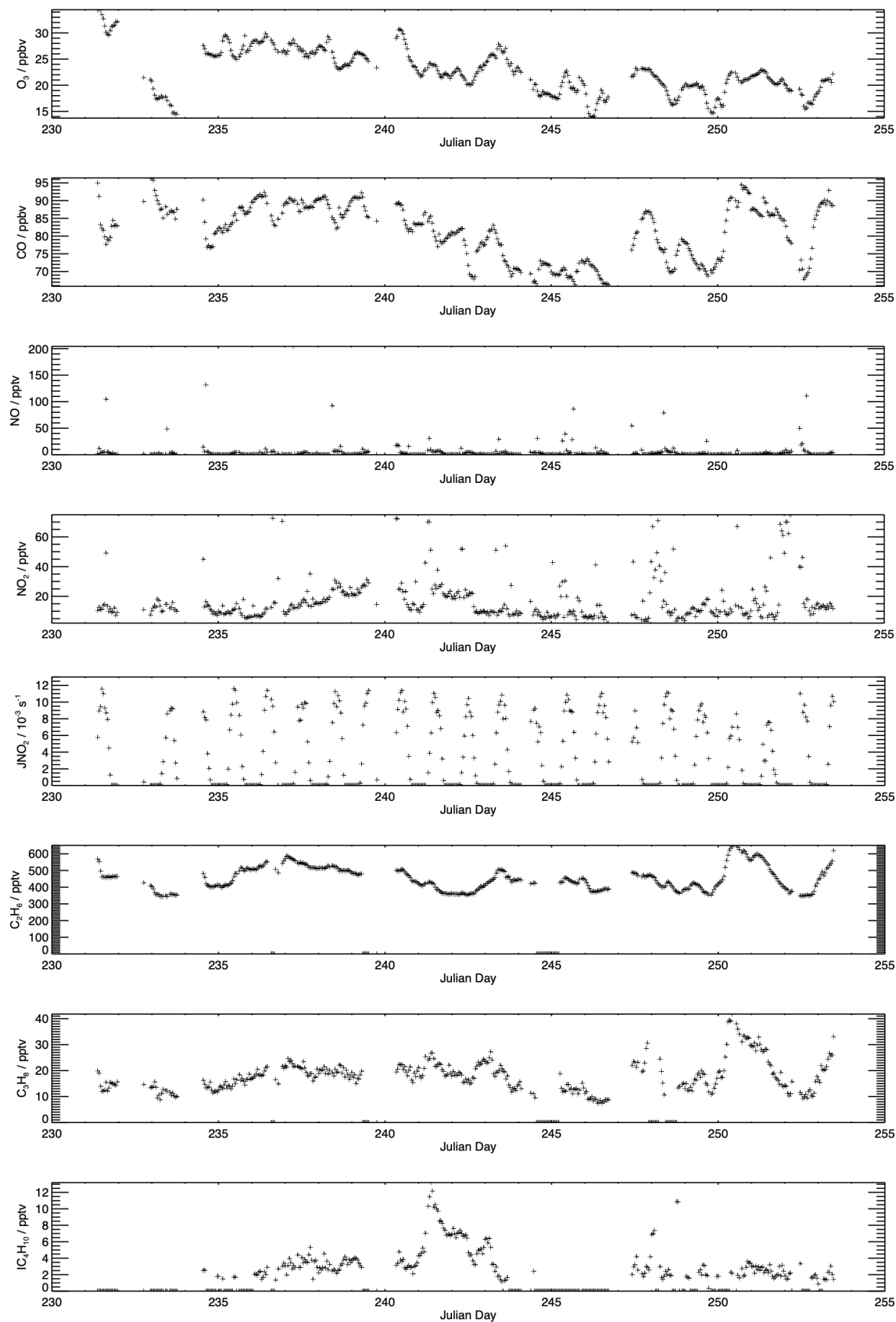


Figure S2: MCM model inputs for campaign 2.

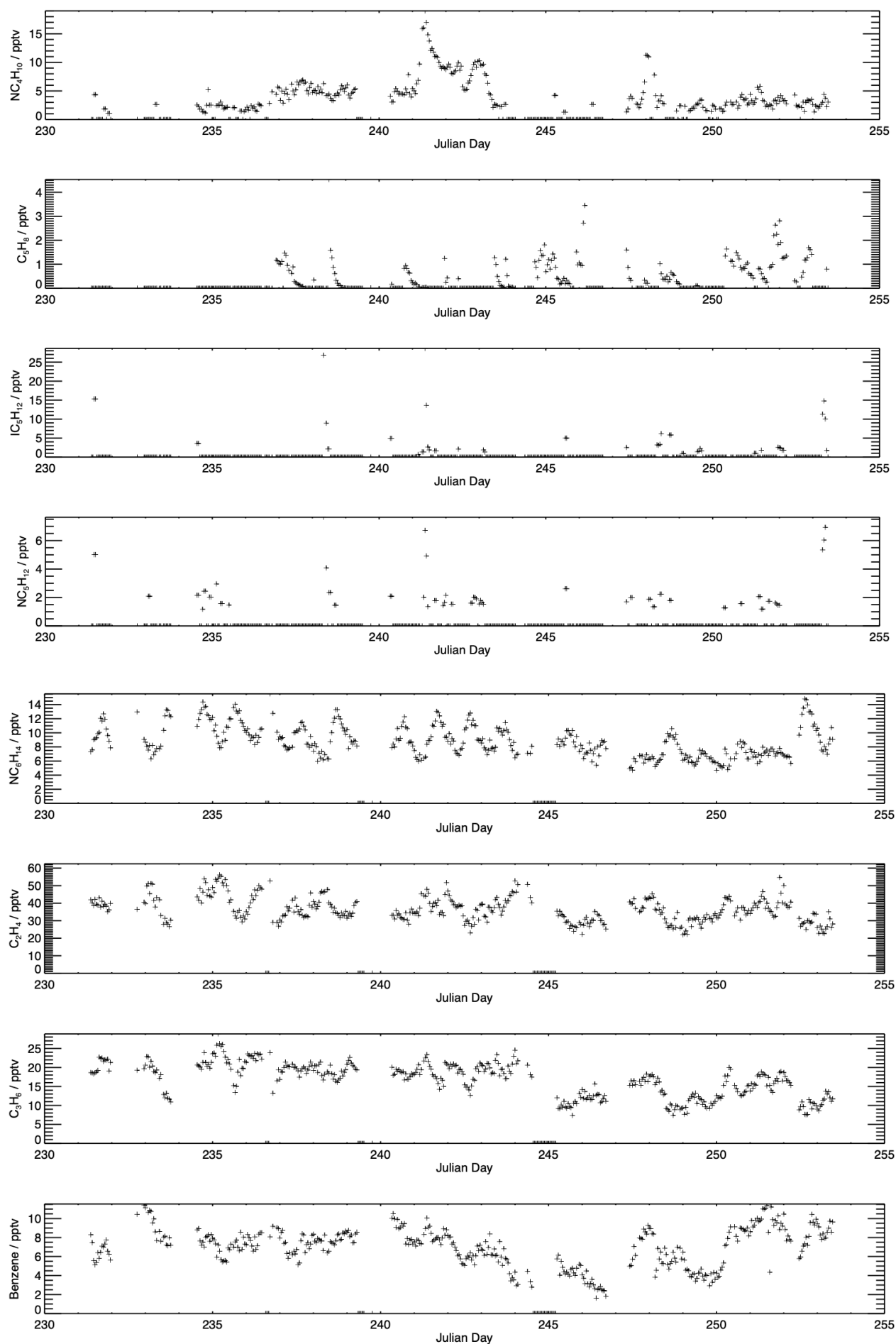


Figure S2: MCM model inputs for campaign 2 (continued).

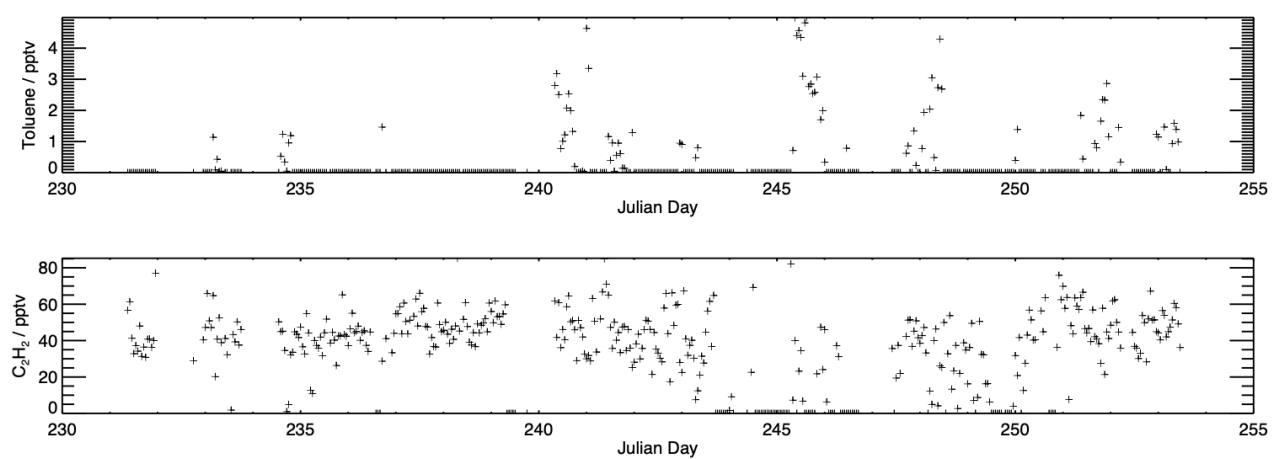


Figure S2: MCM model inputs for campaign 2 (continued).

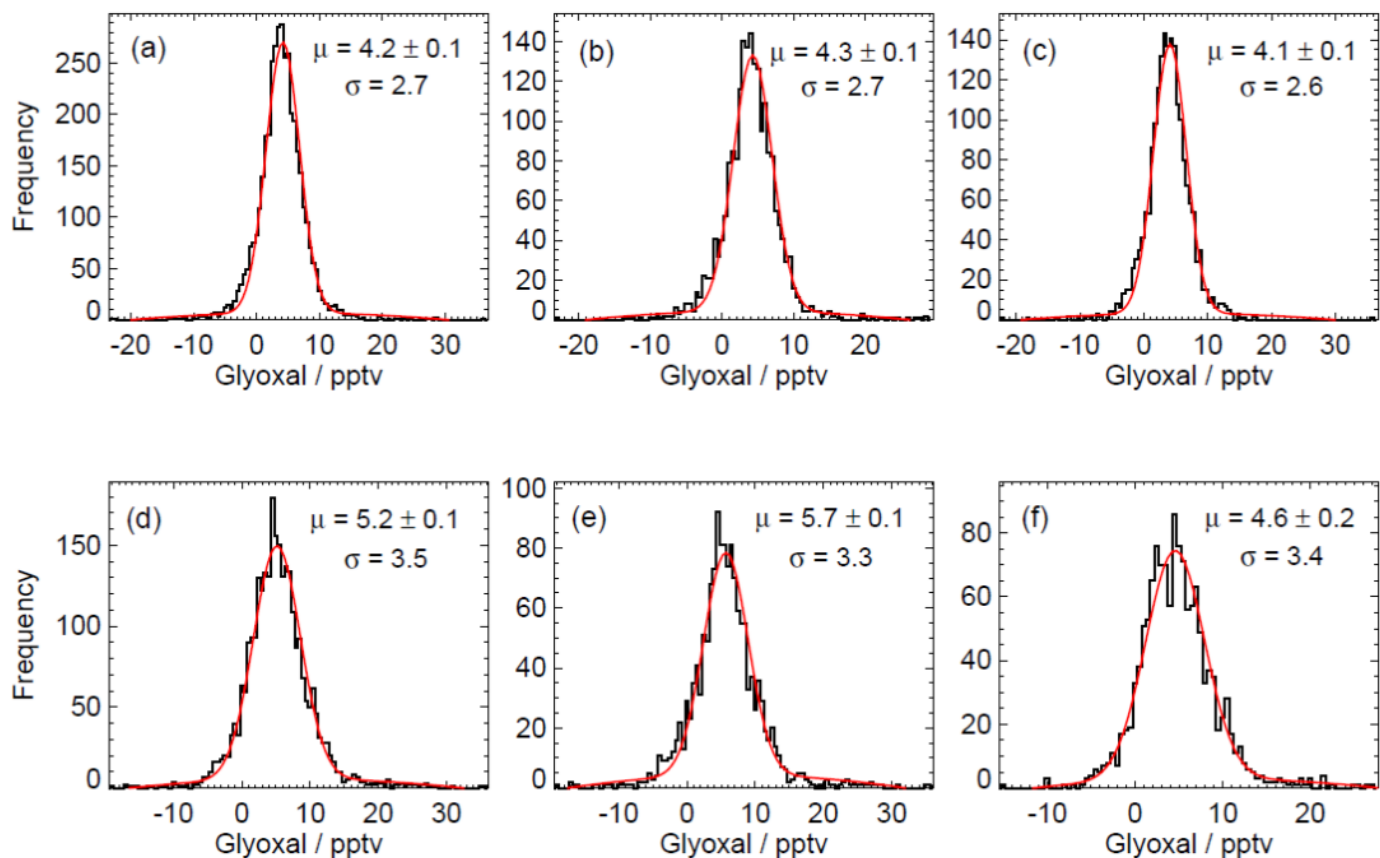


Figure S3: Histograms of glyoxal measurements during (a) all of campaign 1, (b) campaign 1 daytime, (c) campaign 1 nighttime, (d) all of campaign 2, (e) campaign 2 daytime, and (f) campaign 1 nighttime. Red lines show Gaussian curves fit to the data, with the centre and standard deviation given by  $\mu$  and  $\sigma$  respectively.

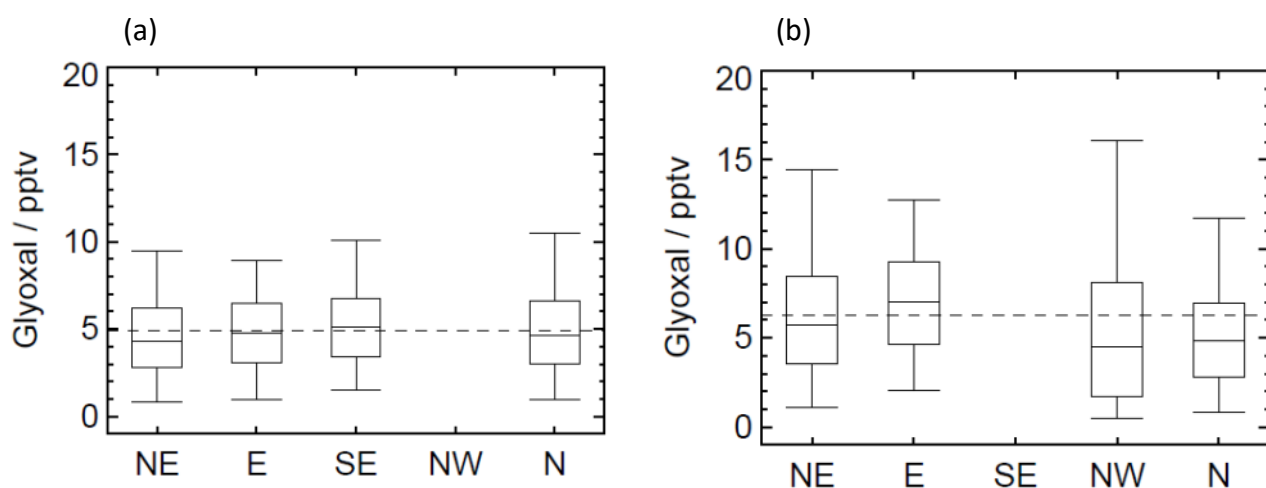


Figure S4: Box and whisker plots of glyoxal measurements categorised by wind direction for (a) campaign 1 and (b) campaign 2. Dashed line indicates campaign mean.



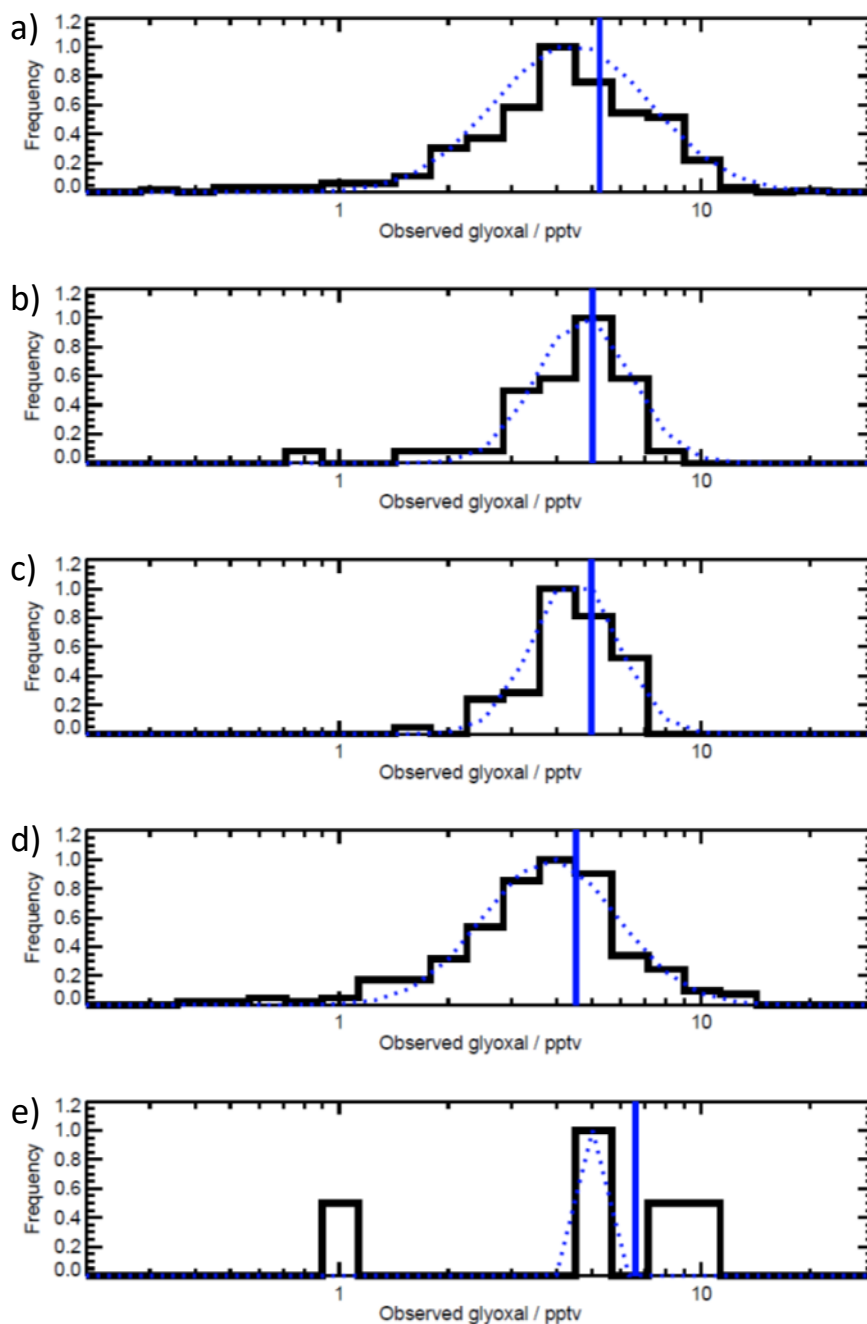


Figure S5: Probability distribution functions of observed glyoxal mixing ratios, separated by air mass origin as indicated by the NAME dispersion model. Dotted blue lines show Gaussian fits to the probability distribution functions. Solid blue lines show the mean glyoxal mixing ratio for a given dataset. Panel (a) corresponds to air masses with African coastal origins; (b) to continental and marine Atlantic origins only; (c) to continental, marine Atlantic and African coastal origins; (d) to European and coastal African origins; (e) to air masses containing dust but not of European origin.

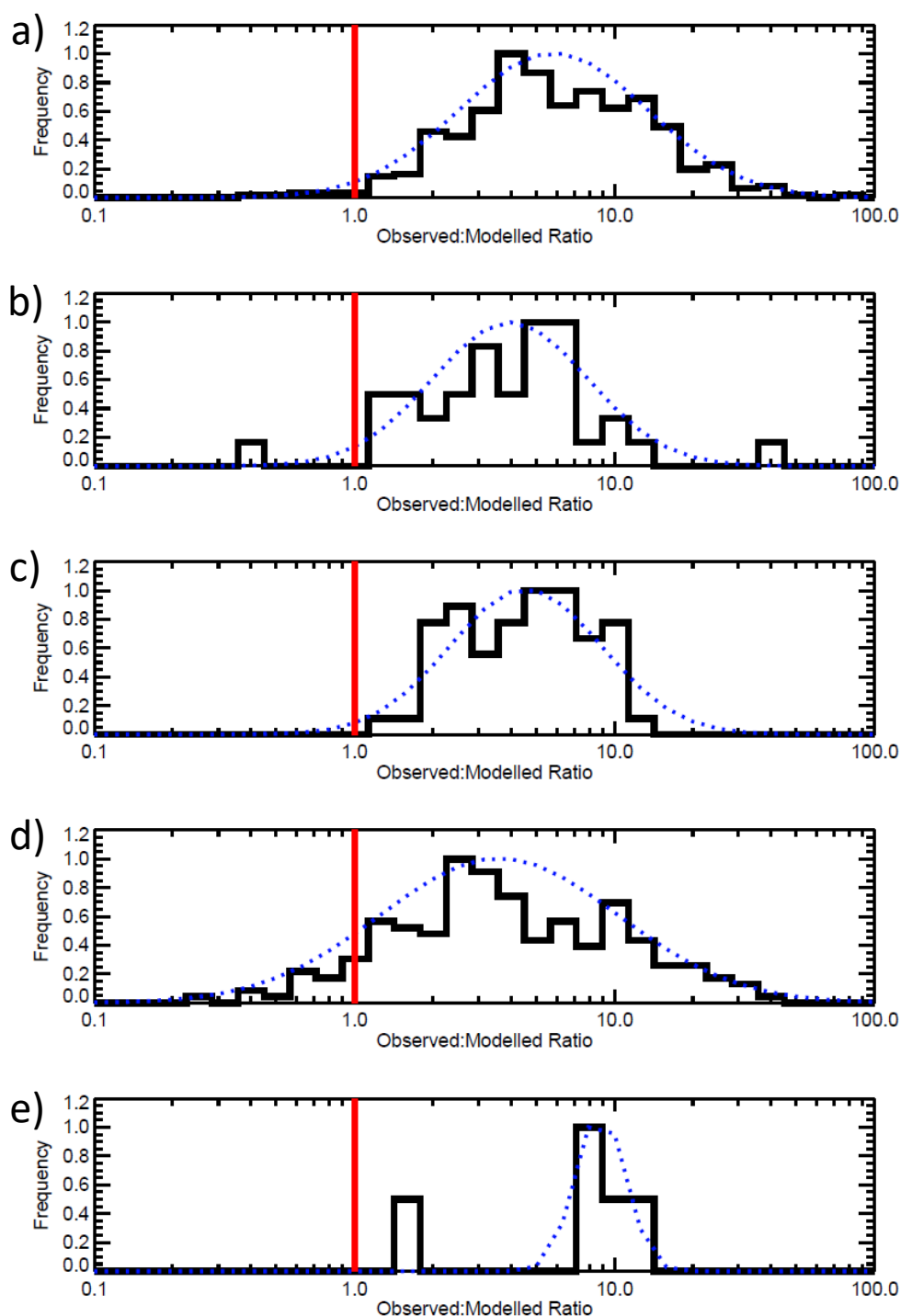


Figure S6: Probability distribution functions of modelled to observed ratios for glyoxal, separated by air mass origin as indicated by the NAME dispersion model. Dotted blue lines show Gaussian fits to the probability distribution functions. Solid red lines show the mean modelled to observed ratio for a given dataset. Panel (a) corresponds to air masses with African coastal origins; (b) to continental and marine Atlantic origins only; (c) to continental, marine Atlantic and African coastal origins; (d) to European and coastal African origins; (e) to air masses containing dust but not of European origin.

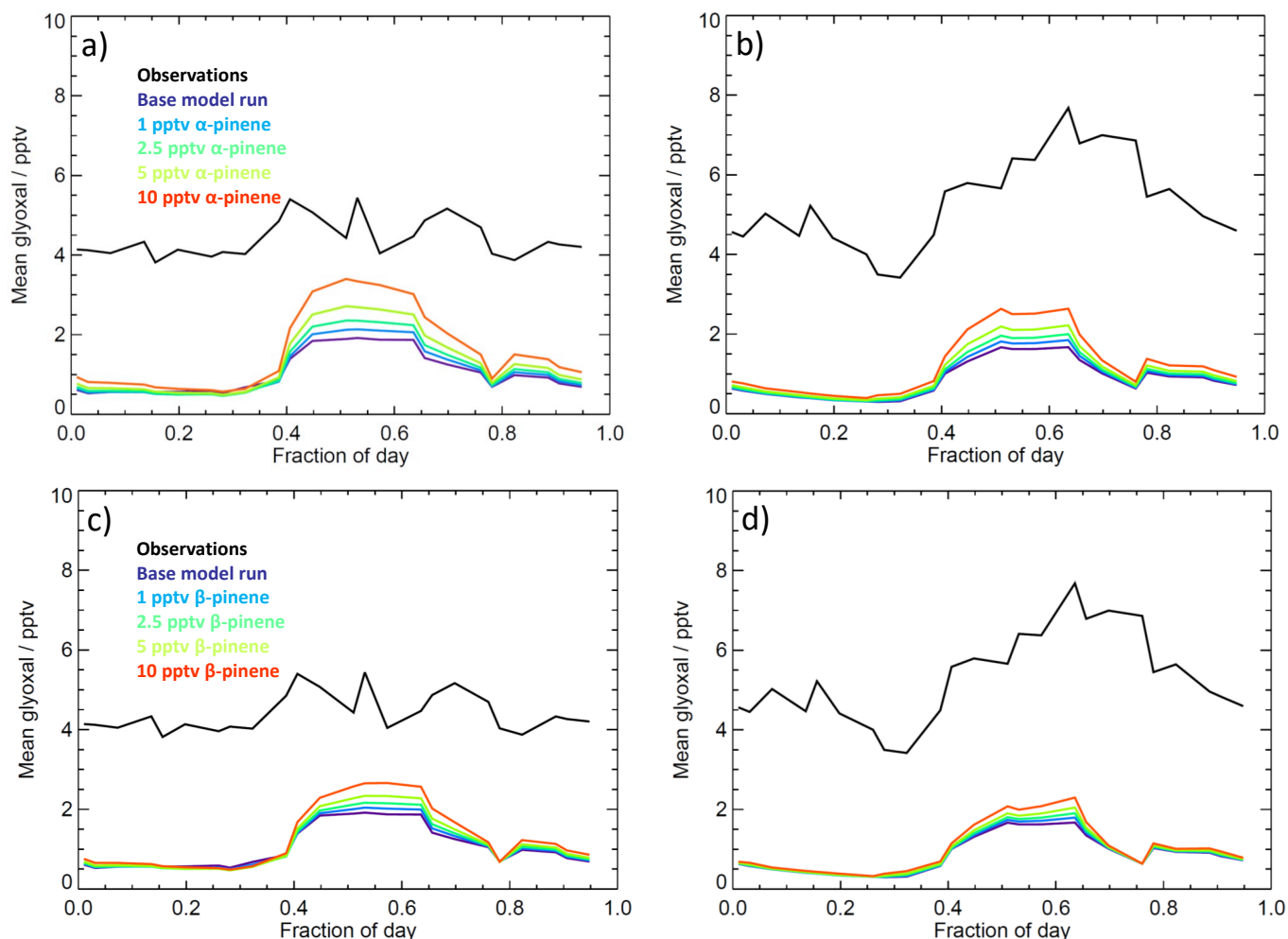


Figure S7: Average observed (black) and modelled glyoxal diurnal profiles showing the sensitivity of the model to monoterpenes for a) the first measurement period with  $\alpha$ -pinene; b) the second measurement period with  $\alpha$ -pinene; c) the first measurement period with  $\beta$ -pinene; d) the second measurement period with  $\beta$ -pinene.

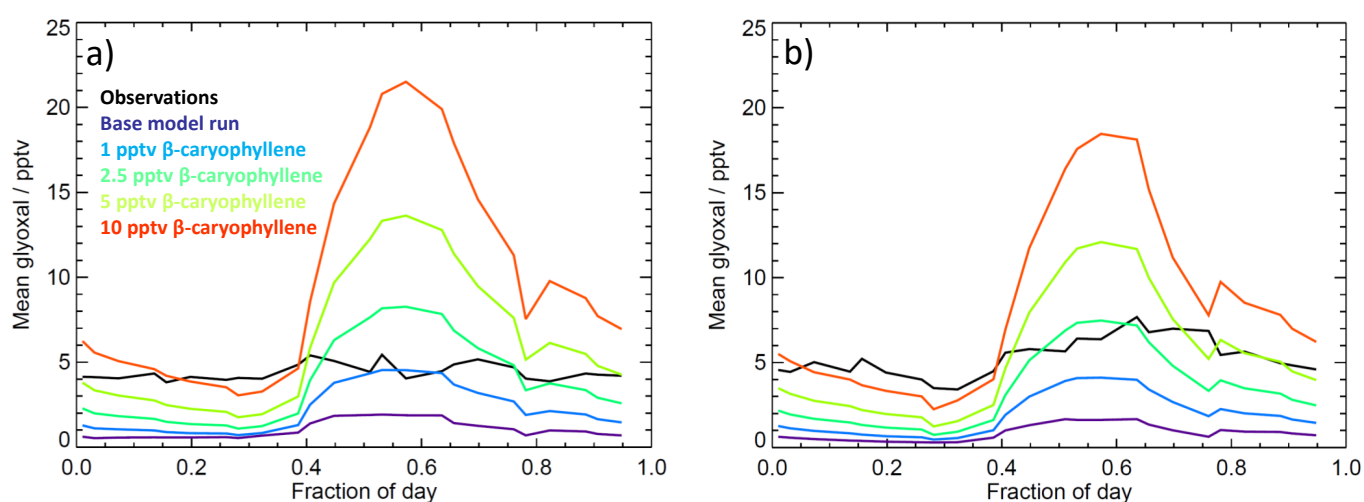


Figure S8: Average observed (black) and modelled glyoxal diurnal profiles showing the sensitivity of the model to the sesquiterpene  $\beta$ -caryophyllene for a) the first measurement period; b) the second measurement period.

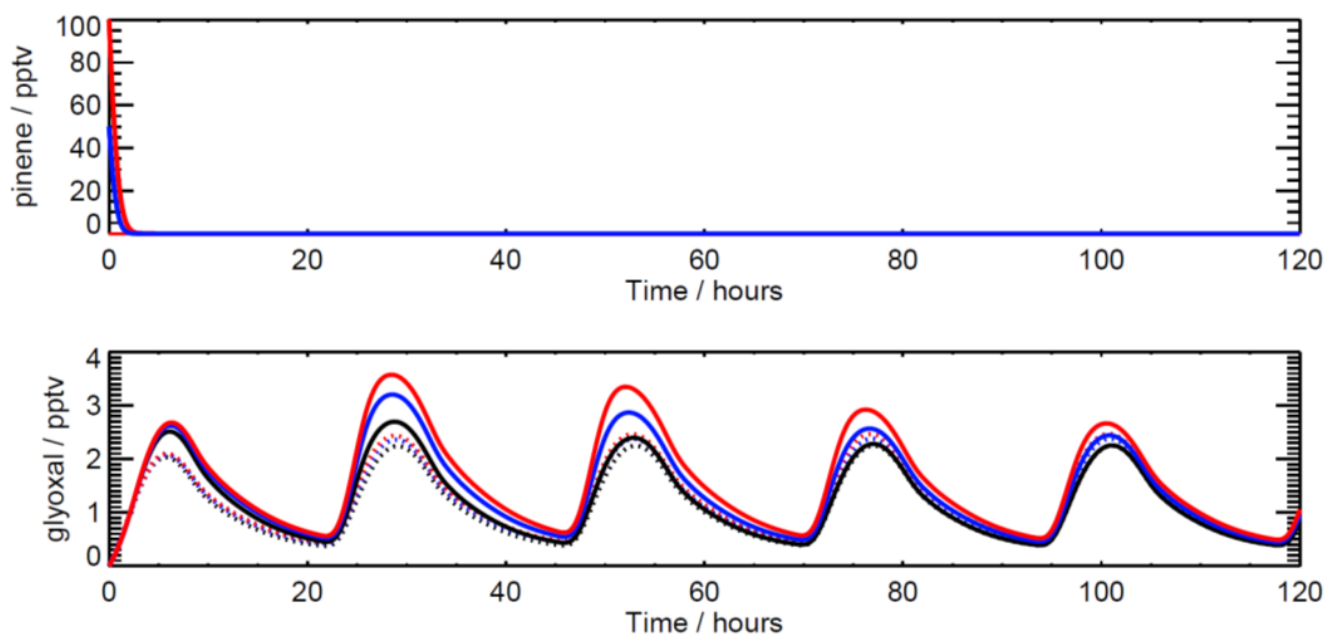


Figure S9: Time profiles for a)  $\alpha$ -pinene (red) and  $\beta$ -pinene (blue) and b) glyoxal for a model run initialised with midday (1000-1400) campaign averages of observed species (for which  $O_3$ ,  $CO$ ,  $H_2O$  and VOC concentrations are constant throughout the model run and  $NO_x$  concentrations constrained but allowed to vary with photochemistry). Broken lines represent model runs constrained to observed species only, solid lines represent model runs in which the model was initialised with 100 pptv  $\alpha$ -pinene and 50 pptv  $\beta$ -pinene input but with the monoterpenes unconstrained throughout the model run to represent the chemical evolution of an air mass passing over an area with high monoterpene emissions, such as a phytoplankton bloom. Line colours represent different deposition lifetimes implemented in the model for model generated intermediates, with standard deposition rates shown in black, deposition rates decreased by a factor of two in blue and deposition rates decreased by a factor of four in red.

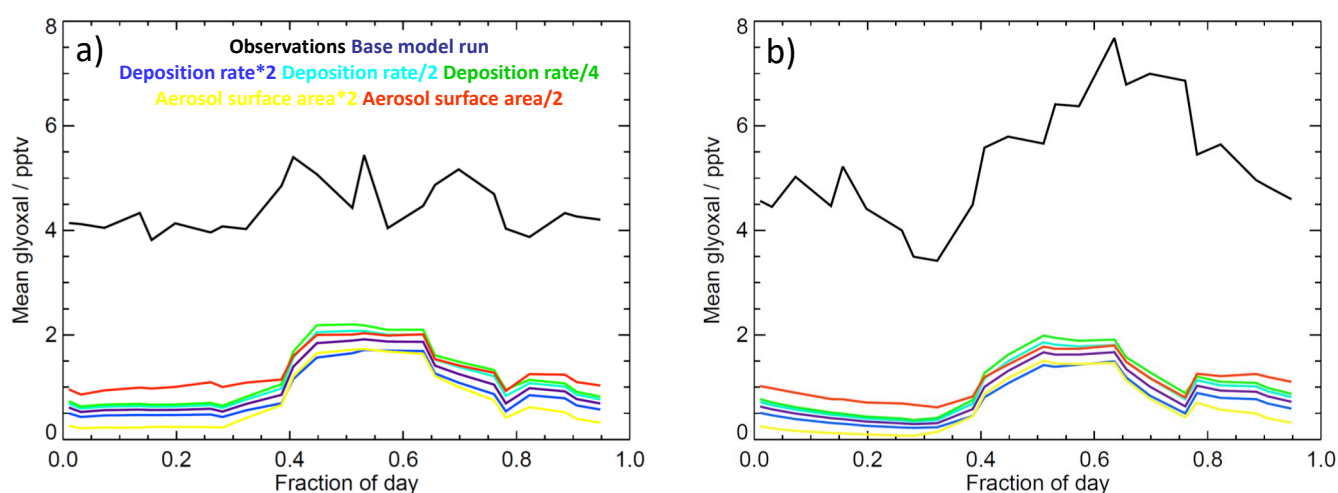


Figure S10: Average observed (black) and modelled glyoxal diurnal profiles showing the sensitivity of the model to deposition rates and aerosol uptake in the model for a) the first measurement period and b) the second measurement period.